14th International Conference on Narrow Gap Semiconductors and Systems

Spin and phase coherence times in Te doped InSb thin films

R.L. Kallaher[a], J.J. Heremans[a]

*[a]Department of Physics, Virginia Tech,
Blacksburg, VA 24061, USA*

Abstract

We investigate the low temperature spin and phase coherence times in Te-doped InSb thin films through measurements of antilocalization. It is found that the extracted spin coherence times range from as long as ~73 ps in films with carrier density $n \approx 0.6 \times 10^{22} \, m^{-3}$ down to ~6 ps for $n \approx 8.9 \times 10^{22} \, m^{-3}$. The dependence on n indicates that the Elliott-Yafet mechanism is responsible for spin decoherence. The measured spin coherence times are in agreement with theoretical predictions when an appropriately weighed momentum scattering time is used. Extracted phase coherence times are inversely proportional to temperature, consistent with phase decoherence via the Nyquist mechanism.

Keywords: antilocalization, magnetoresistance, spin coherence, InSb, spintronics

1. INTRODUCTION

We examine the spin coherence time τ_{so} and phase coherence time τ_{φ} in thin films of n-InSb with different electron densities (n) at temperatures $T \leq 10 \, K$. Values for τ_{so} and τ_{φ} are obtained by analyzing the low-field magnetoresistance in antilocalization theory [1, 2, 3, 4, 5, 6]. In materials with strong spin-orbit interactions, quantum interference between electrons on exact time reversed trajectories leads to antilocalization (AL), and results in a sharp positive magnetoresistance around zero applied magnetic field (H=0), which crosses over to negative magnetoresistance at higher H. The crossover field is largely determined by $1/\tau_{so}$, whereas the magnitude of the positive magnetoresistance is related to the ratio τ_{φ}/τ_{so}. This allows quantitative information about τ_{so} and τ_{φ} to be extracted from the magnetoresistance [1, 2, 3, 4, 5, 6] and AL has become a valuable tool for examining both τ_{so} [4, 5, 6, 7, 8, 9, 10, 11, 12] and τ_{φ} [6, 7, 8, 9, 13] in semiconducting systems.

Email addresses: `kallaher@vt.edu` (R.L. Kallaher), `heremans@vt.edu` (J.J. Heremans)

Table 1: Layer structure and transport properties at $T = 0.4\ K$ for the different InSb film types: buffer layer thickness (t_{Buffer}) and Te doping ($N_{D,Buffer}$, UD=undoped); active layer thickness (t) and Te doping (N_D); cap layer thickness (t_{Cap}) and Te doping ($N_{D,Cap}$); electron density (n); mobility (μ); Fermi energy (E_F).

	A	B	C
t_{Buffer} (μm)	0.2	0.15	0.2
$N_{D,Buffer}$ ($10^{22} m^{-3}$)	UD	UD	4
$t(active)$ (μm)	1.3	0.6	1.3
$N_D(active)$ ($10^{22} m^{-3}$)	2	3	10
t_{Cap} (μm)	0.05	0.05	0.05
$N_{D,Cap}$ ($10^{22} m^{-3}$)	15	15	30
n ($10^{22} m^{-3}$)	0.6 - 0.7	2.8 - 3.1	8.8 - 9.0
μ (m^2/Vs)	4.0 - 4.4	3.4 - 3.5	4.4 - 4.5
E_F (meV)	8.3 - 9.2	22.0 - 23.4	43.5 - 44.1

2. EXPERIMENT

Low-field magnetoresistance measurements were performed on high mobility (μ) Te-doped InSb thin films. Each MOCVD-grown film is composed of three distinct InSb layers. Electrical transport through the film is dominated by the high μ active layer which is positioned between a buffer and cap layer. The buffer layer allows for higher μ in the active layer by mitigating the effects arising from the 14% lattice mismatch between the GaAs ⟨100⟩ substrate and InSb. A low μ, heavily doped 0.05 μm cap layer facilitates Ohmic contacts to the active layer. The thickness and doping level of the buffer, active, and cap layers for the different InSb films are summarized in Table 1. Further details about the structure and transport properties of these films are presented and discussed elsewhere [7, 14, 15]. These previous studies have revealed that the active layer has much larger average μ as compared to either the buffer or cap layer and that scattering by charged impurities limits μ at low T [14, 15]. Based on the relative doping, thickness, and average μ of the different layers, a multilayer in-plane magnetotransport analysis suggests that the active layer conducts ~95% of the overall current [7, 16]. Thus, the magnetotransport is assumed to be dominated by the active layer only, and contributions from the buffer and cap layers are neglected. Hall and zero field resistivity (ρ_0) measurements were performed in order to characterize the electron mobility μ and electron density n at low T, as collected in Table 1.

Examples of the observed magnetoresistance are shown in Fig. 1. The component antisymmetric with respect to H has been subtracted from the raw data in order to remove contributions from the Hall effect and any slight electronic drifts. Antilocalization is observed in all the measured films. The field at which the positive to negative magnetoresistance crossover occurs is lower for films with smaller density, indicating that τ_{so} is largest in the lower doped films. In addition, it is noted that in each of the films the crossover field remains relatively constant as a function of T. However, the magnitude of the positive magnetoresistance rapidly decreases with increasing T. This suggests that in this range of T, τ_{so} exhibits little or no T-dependence and that the T-dependence of the low-field magnetoresistance is dominated by the behavior of τ_{φ}.
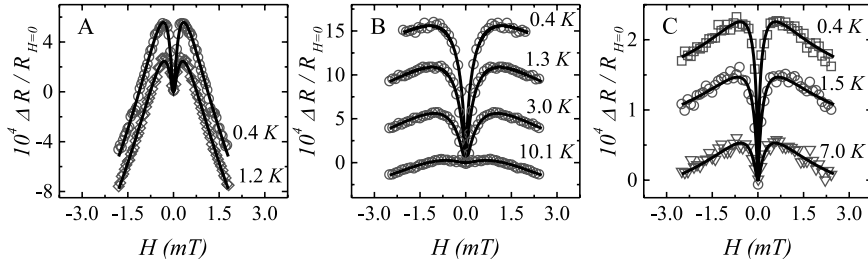
Figure 1: Examples of the measured low H magnetoresistance at variable T, along with theoretical models based on Eq. (1) (black lines), for the InSb film types A, B, C.

3. ANALYSIS

In order to obtain quantitative information about τ_{so} and τ_φ, the magnetoresistance traces were fit to an AL theory that includes the effects of spin-orbit interactions. The quantum corrections to the conductivity arising from AL are sensitive to the mobilitiy scattering time τ_p, diffusion constant D, magnetic scattering time τ_s, spin coherence time τ_{so}, and phase coherence time τ_φ. However, since the InSb films are free from magnetic impurities, τ_s is neglected in the analysis of the magnetoresistance curves. Using values of n and μ obtained from ρ_0 and Hall measurements, we calculate $\tau_p = m^*\mu/e$ and $D = \frac{1}{3}v_F^2\tau_p$, taking the nonparabolicity of the InSb conduction band into account for the effective mass m^* and Fermi velocity v_F [17].

In thin films of thickness t, phase coherent phenomena, such as AL, display two-dimensional behavior when the phase coherence length $L_\varphi = \sqrt{D\tau_\varphi} > t$ [18]. We find that fitting the data with AL theory self-consistently yields an $L_\varphi > t$ for all T at which AL was experimentally observed. Therefore, the magnetoresistance curves are modeled with a two-dimensional localization theory [3]. For isotropic spin-orbit scattering, the corrections to the resistivity in perpendicular H are given by [2, 3, 18]:

$$\frac{-\Delta\rho}{\rho_0^2} \approx \Delta\sigma = \frac{-e^2}{2\pi^2\hbar}\left[\Psi\left(\frac{1}{2}+\frac{H_{tr}}{H}\right)+\frac{1}{2}\Psi\left(\frac{1}{2}+\frac{H_\varphi}{H}\right)-\frac{3}{2}\Psi\left(\frac{1}{2}+\frac{H_\varphi}{H}+\frac{4}{3}\frac{H_{so}}{H}\right)\right] \qquad (1)$$

where Ψ is the digamma function, $H_{tr} = \hbar/\left(4eD\tau_p\right)$, $H_\varphi = \hbar/\left(4eD\tau_\varphi\right)$ and $H_{so} = \hbar/\left(4eD\tau_{so}\right)$. With τ_p and D predetermined, the magnetoresistance traces at each T were independently fit to Eq. (1) in order to determine both τ_{so} and τ_φ. The results of these fits are plotted along with the experimental data in Fig. 1. Extracted values for τ_{so} and τ_φ are presented and discussed below.

4. RESULTS

4.1. Spin coherence time

Extracted values of τ_{so} for the three different film types are displayed in Fig. 2. Similar to τ_p, it is observed that τ_{so} displays an only weak dependence on T for $0.4\,K < T < 10\,K$. τ_{so} does, however, exhibit a strong dependence on n, with τ_{so} varying from $\sim 6\,ps$ for $n \approx 8.9\,x\,10^{22}\,m^{-3}$ to $\sim 73\,ps$ for $n \approx 0.6\,x\,10^{22}\,m^{-3}$. The corresponding spin coherence lengths $L_{so} = \sqrt{D\tau_{so}}$ are also illustrated in Fig. 2. We find $L_{so} \geq 0.9\,\mu m$, with L_{so} as long as $1.5\,\mu m$ in sample type A.
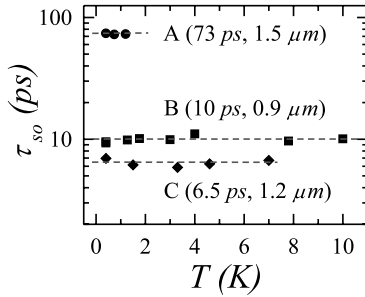
Figure 2: Spin coherence times τ_{so} *vs* T, obtained from the fits of Eq. (1) to the data in Fig. 1. Dashed horizontal lines indicate average values of τ_{so}, also in parentheses with the spin coherence length L_{so}.
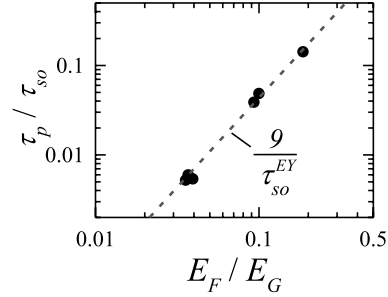
Figure 3: Logarithmic plot of the spin decoherence rate, $1/\tau_{so}$ (normalized to $1/\tau_p$, see text). The dashed line shows that the experimental $1/\tau_{so}$ is 9 times larger than $1/\tau_{so}^{EY}$ as predicted from Eq. (2) using τ_p.

The spin-orbit scattering mechanisms which determine spin decoherence in n-type InSb thin films are the D'yakonov-Perel (DP) mechanism [19, 20, 21, 22] and the Elliott-Yafet (EY) mechanism [19, 20, 21, 23, 24]. For degenerate bulk semiconductors, the spin relaxation rates under the EY and DP mechanisms depend on the semiconductor's band gap E_G, spin-orbit splitting of its valence bands Δ, and Fermi energy E_F. Theoretically these rates are given by [19, 20, 21, 25]:

$$\frac{1}{\tau_{so}^{EY}} = \frac{\alpha_{EY}}{\tau_p}\gamma^2\left(\frac{1-\gamma/2}{1-\gamma/3}\right)^2\left(\frac{E_F}{E_G}\right)^2, \quad \frac{1}{\tau_{so}^{DP}} \cong \alpha_{DP}\left(\frac{E_F^3}{\hbar^2 E_G}\right)\frac{\gamma^2}{3-\gamma}\left(\frac{m^*}{m_0}\right)^2\tau_p \quad (2)$$

where m_0 represents the free electron mass, and $\gamma = \Delta/(\Delta + E_G)$ ($\Delta = 810\,meV$ and $E_G = 236\,meV$ in InSb at low T [26]). $\alpha_{EY,DP}$ are constants which depend on the dominant scattering mechanism [19, 20, 21]. Because $1/\tau_{so} \sim E_F^\nu$ for both EY ($\nu = 2$) and DP ($\nu = 3$) mechanisms, a logarithmic plot of $1/\tau_{so}$ *vs* E_F can distinguish which mechanism dominates spin decoherence. Although the DP mechanism dominates spin decoherence in many other n-type III-V materials and heterostructures [27, 28], the EY mechanism can be relevant in InSb systems [19, 20, 21, 25, 29].

Figure 3 depicts the dependence of $1/\tau_{so}$ on E_F, with τ_{so} given in units of τ_p in order to allow for the different μ in each of the films. The logarithmic plot shows $\tau_{so} \sim E_F^{-2}$, consistent with spin decoherence via the EY mechanism. For scattering by charged impurities, $\alpha_{EY}=32/27$ [19, 20, 21, 25]. Thus, with τ_p as the measure of the timescale over which itinerant electrons are scattered, Eq. (2) would predict a decoherence rate $1/\tau_{so}^{EY}$ that is a factor ~ 9 smaller than what is experimentally observed. This indicates that the appropriate scattering timescale for spin decoherence under the EY mechanism is different than the timescale governing momentum relaxation. Predictions based on τ_p, which is disproportionately sensitive to backscattering, can thus underestimate the spin decoherence rate. We note that for calculations of spin relaxation resulting from the cubic Dresselhaus spin-orbit term in bulk semiconductors [28], τ_3 is the relevant scattering timescale, where τ_3 is defined by: $\tau_3^{-1} = \int_{-1}^{1} W(\theta)\left[1 - P_3(\cos(\theta))\right]d\cos(\theta)$. Here $W(\theta)$ denotes the θ-dependent scattering probability, and P_3 the 3rd Legendre polynomial. Calculations show that $\tau_3/\tau_p \approx 1/6$ for charged impurity scattering [7, 19, 20, 21] and thus sub-
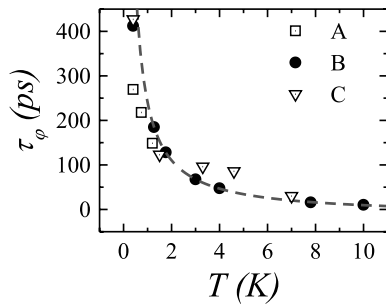
Figure 4: Extracted phase coherence times τ_φ *vs* T, obtained from the fits of Eq. (1) to the data in Fig. 1. Dashed line indicates a fit to a $1/T$ dependence for sample B.

stituting $\tau_3 \rightarrow \tau_p$ in Eq. (2) brings theoretical predictions of τ_{so}^{EY} within a factor 1.5 of experimental observations.

4.2. Phase coherence time

As compared to τ_{so}, a strong T-dependence of τ_φ is observed (Fig. 4). For samples B and C, τ_φ is found to decrease by more than an order of magnitude as T is increased from $0.4\,K$ to $\sim 8\,K$. With a constant τ_{so}, the changes in τ_φ are responsible for the observed T-dependence of the low-field magnetoresistance, as the magnitude of the AL corrections are related to the ratio of τ_φ / τ_{so}. Thus, as τ_φ decreases with increasing T, the magnitude of the AL corrections diminish and as a consequence AL is observed over a larger range of T in films with small values of τ_{so}. It is found that $\tau_\varphi \sim 1/T$ in samples B and C. The T-dependence of sample A is not independently evaluated as the long τ_{so} limits the range of T over which AL is observed. The $1/T$ dependence of τ_φ is characteristic of phase decoherence via the Nyquist electron-electron dephasing mechanism [8, 30, 31, 32]. The dashed line in Fig. 4 explicity depicts the $1/T$ dependence of τ_φ in sample B. The data follow this $1/T$ behavior except at the lowest $T = 0.4\,K$ where saturation of τ_φ is observed. The tendency for τ_φ to saturate towards a constant value as $T \rightarrow 0$ is often observed in experimental studies of τ_φ [32] and indicates the presence of additional phase-breaking mechanisms [2, 8, 32, 33].

5. CONCLUSIONS

In summary, we have examined spin and phase coherence in high quality Te-doped InSb thin films through measurements of AL. It is observed that $1/\tau_{so} \sim E_F^2$ indicating that the spin decoherence is dominated by the EY mechanism. Even though the experimental spin coherence times are shorter than predicted by the EY model, the inherently large μ in InSb allows for considerable spin coherence lengths; $L_{so} \geq 0.9\,\mu m$ is observed. Phase coherence times follow $\tau_\varphi \sim 1/T$, typical of the Nyquist electron-electron dephasing mechanism. This work was supported by DOE through grant DE-FG02-08ER46532 and NSF through grant DMR-0618235.

References

[1] B. L. Al'tshuler, A. G. Aronov, A. I. Larkin, Sov. Phys. JETP 54 (1981) 411.

[2] G. Bergmann, Phys. Rep. 107 (1984) 1.
[3] S. Hikami, A. I. Larkin, Y. Nagaoka, Prog. Theor. Phys. 63 (1980) 707.
[4] A. Zduniak, M. I. Dyakonov, W. Knap, Phys. Rev. B 56 (1997) 1996.
[5] W. Knap, C. Skierbiszewski, A. Zduniak, E. Litwin-Staszewska, D. Bertho, F. Kobbi, J. L. Robert, G. E. Pikus,
      F. G. Pikus, S. V. Iordanskii, V. Mosser, K. Zekentes, Y. B. Lyanda-Geller, Phys. Rev. B 53 (1996) 3912.
[6] J. B. Miller, D. M. Zumbühl, C. M. Marcus, Y. B. Lyanda-Geller, K. C. D. Goldhaber-Gordon, A. C. Gossard,
      Phys. Rev. Lett. 90 (2003) 076807.
[7] R. L. Kallaher, J. J. Heremans, Phys. Rev. B 79 (2009) 075322.
[8] S. A. Studenikin, P. T. Coleridge, N. Ahmed, P. J. Poole, A. Sachrajda, Phys. Rev. B 68 (2003) 035317.
[9] D. D. Bykanov, A. M. Kreshcuk, S. V. Novikov, T. A. Polyanskaya, I. G. Savel'ev, Semiconductors 32 (1998) 985.
[10] T. Koga, J. Nitta, T. Akazaki, , H. Takayanagi, Phys. Rev. Lett. 89 (2002) 046801.
[11] M. Oszwaldowski, T. Berus, V. K. Dugaev, Phys. Rev. B 65 (2002) 235418.
[12] S. Ishida, K. Takeda, A. Okamoto, I. Shibasaki, Physica E 20 (2004) 211.
[13] S. McPhail, C. E. Yasin, A. R. Hamilton, M. Y. Simmons, E. H. Linfield, M. Pepper, D. A. Ritchie, Phys. Rev. B
      70 (2004) 245311.
[14] M. W. Pelczynski, J. J. Heremans, S. Schwed, Mater. Res. Soc. Symp. Proc. 607 (2000) 65.
[15] D. L. Partin, M. Pelczynski, P. Cooke, L. Green, J. Heremans, C. Thrush, J. Cryst. Growth 195 (1998) 378.
[16] R. L. Petritz, Phys. Rev. 110 (1958) 1254.
[17] W. Zawadzki, W. Szymanska, Phys. Stat. Sol. B 45 (1971) 415.
[18] S. Kobayashi, F. Komori, Prog. Theor. Phys. Suppl. 84 (1985) 224.
[19] G. E. Pikus, A. N. Titkov, Optical Orientation, North-Holland, Amsterdam, 1984.
[20] I. Zutic, J. Fabian, S. D. Sarma, Rev. Mod. Phys. 76 (2004) 323.
[21] P. H. Song, K. W. Kim, Phys. Rev. B 66 (2002) 035207.
[22] M. I. D'yakonov, V. I. Perel', Sov. Phys. JETP 33 (1971) 1053.
[23] R. J. Elliott, Phys. Rev. 96 (1954) 266.
[24] Y. Yafet, Solid State Physics, vol. 14, Academic, New York, 1963.
[25] J. N. Chazalviel, Phys. Rev. B 11 (1975) 1555.
[26] O. Madelung, Semiconductors: Data Handbook, 3rd Ed., Springer, Berlin, 2004.
[27] J. Kainz, U. Rössler, R. Winkler, Phys. Rev. B 70 (2004) 195322.
[28] W. H. Lau, J. T. Olesberg, M. E. Flatté, Phys. Rev. B 64 (2001) 161301(R).
[29] K. L. Litvinenko, L. Nikzad, J. Allam, B. N. Murdin, C. R. Pidgeon, J. J. Harris, T. Zhang, L. F. Cohen, J. Appl.
      Phys. 101 (2007) 083105.
[30] B. L. Altshuler, A. G. Aronov, D. E. Khmelnitskii, J. Phys. C 15 (1982) 7367.
[31] A. G. Huibers, M. Switkes, C. M. Marcus, K. Campman, A. C. Gossard, Phys. Rev. Lett. 81 (1998) 200.
[32] J. J. Lin, J. P. Bird, J. Phys: Condens. Matter 14 (2002) R501 and refs. therein.
[33] P. Mohanty, E. M. Q. Jariwala, R. A. Webb, Phys. Rev. Lett. 78 (1997) 3366.